Nano-scale characterization of dielectric-semicon contacts

Francesco Gullo, Christina Villeneuve-Faure, Séverine Le Roy, Christian Laurent, Gilbert Teyssedre, T. Christen, C. Törnkvist, H. Hillborg

Nano-scale characterization of insulator-semicon contacts

F. Gullo*, C. Villeneuve-Faure, S. Le Roy, C. Laurent, G. Teyssedre

LAPLACE, Université de Toulouse, CNRS, INPT, UPS
* Corresponding author: gullo@laplace.univ-tlse.fr

T.Christen[1], C.Törnkvist[2], H. Hillborg[2]

ABB Corporate Research
CH-5405, Baden, Switzerland[1]
SE-72178, Vasteras, Sweden[2]

***Abstract*— A main challenge in the development of polymer-insulated HVDC power cables is to achieve a robust insulation, because the accumulation of space charge under electrical and/or thermal stresses can significantly reduce the cable reliability. The space charge formation depends on the electrode-insulation contact which refers to the transition of carbon-black filled host polymer ('semicon', SC) and unfilled polymer. The fundamental processes which govern the contact physics and their dependence on the microstructure properties of the polymer and the interface are still poorly understood. In this paper we present a methodology to probe SC-insulator contact properties on a nanometer scale and to investigate the impact of material processing.**

Keywords—Polymer; HVDC cable insulation, electrical contact, atomic and Kelvin probe micrsocopy

I. INTRODUCTION

The development of HVDC cable technology faces the problem of material design and optimization in a context where phenomena that play a role in dielectrics under DC stress are far from being under control [1][2]. Contrary to AC stress, where the electric field distribution is governed by the permittivity, under DC, it is essentially controlled by resistivity or conductivity [3]. The resistivity in dielectrics is temperature and field dependent (in contrast to the much less dependent dielectric permittivity). Therefore, the electric field distribution under DC stress is largely determined by the operating conditions. In particular, space charge effects may change the contact behavior dependent on the interface type (metal/insulator, semicon/ insulator, dielectric/ insulator) and make difficult to estimate the electric field distribution both in transient and steady state conditions [4]. The prediction of the field distribution is, however, the most important pre-requisite for designing insulation devices like cables and cable accessories (i.e. joints and terminations).

Progress in this frame can be carried out by systematic materials characterization through space charge or conductivity measurements [3] for understanding and modelling, which provides help towards greater control of the HVDC insulation behavior. However, in order to take into account the processes at the interfaces, boundary conditions need to be settled [4]. Such boundary conditions encompass for example charges exchange at metal/electrode interface [5], or possibly electrochemical processes due to ion drift from the bulk to the surface [6]. Since, in extra clean insulation, the majority carriers are not intrinsic but usually injected, it is obvious that the conductance of insulation is strongly governed by the contact boundary conditions. To determine them, the electrode-insulator interface properties must be known. Unfortunately, space charge measurement methods like Pulsed Electro Acoustic (PEA) method [8], which may provide spatial information, exhibit an upper limit of the resolution of a few microns, which is insufficient for reasonable interface characterization.

This article discusses appropriate methodologies for understanding the semicon (SC) - polymer insulation contact properties with the help of Fourier Transform Infrared (FTIR) Spectroscopy, Atomic Force Microscopy (AFM) and Kelvin Probe Force Microscopy (KPFM).

II. MATERIALS AND EQUIPMENT

A. Sample preparation

The materials were chosen to minimize the complexity of the matter. As a base insulation material we used a non-stabilized low-density polyethylene from ExxonMobil™ (LDPE LD 101BA), which is designed for Medium/High Voltage insulation, and which can be peroxide crosslinked.

To avoid that contact properties be influenced by diffusion of additives and impurities, the SC was produced by adding to the LDPE carbon black (CB) nanoparticles compressed into granules. The CB is an acetylene black compound for electrical applications (Denka Black 50%). The mixing was done with a Brabender internal mixer for 15 minutes at 15 rpm and 130°C with a ratio of 50/50 wt.% LDPE/CB.

These materials are used to realize sandwich-like samples in 3 layers SC-LDPE-SC (3x50µm) through steps depicted in Fig. 1. Each single layer is produced in a hot-press by heating at 140°C and compressing the proper amount of pellets in the mold. To avoid that these films stick to the mold surface, a covering layer is used. Previous studies suggest that the material used for this cover layer induces different properties on the film [9][10]. For this reason, we will compare samples produced with aluminum and produced with PET (Mylar) as cover layer. The single layer films can be analyzed in this form or represent the first step to make the sandwich SC-LDPE-SC (Fig.1a). By using a special mask, the three layers can be melted

Cite as: F. Gullo, T. Christen, C. Villeneuve-Faure, C. Törnkvist, S. Le Roy, H. Hillborg, C. Laurent, G. Teyssedre, "*Nano-scale characterization of dielectric-semicon contacts*", IEEE Int. Conf. on Dielectrics (ICD), Montpellier, 3-7 July 2016. Proc. ICD, pp. 796-799, **2016**. DOI: 10.1109/ICD.2016.7547735

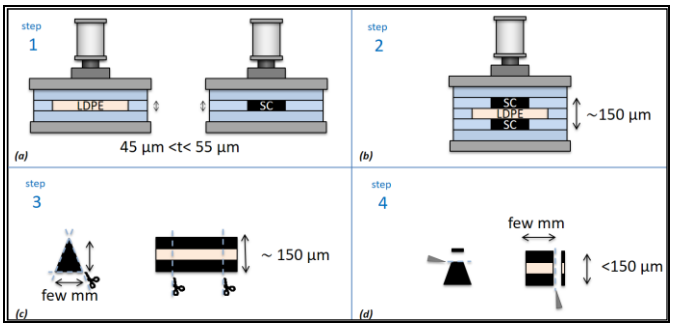

Fig. 1. The four steps for the realization of a sandwich SC-LDPE-SC for AFM measurement in cross-section: (a) press of the single layers; (b) agregation of the three layers; (c) cut of a small triangle; (d) cut a tip with an ultra-cryo-microtome to obtain a flat surface. The cover layer coloured in light blue in (a-b), depending on the sample, is made of aluminum or PET.

together with heating to 110° C and applying a small pressure (Fig.1b). In this manner, samples with two flat LDPE-SC contacts are produced. To analyze this sample in cross-section, it is cut a small triangle, as shown in Fig.1c. Using an ultra-cryo-microtome a flat surface about 150µm width and few hundred microns length is obtained from the tip of the triangle by removing thin layers of about 200 nm in thickness (Fig.1d). After this treatment the surface is flat enough to measure the contact properties in cross-section.

B. *Equipement*

Different techniques were used to characterize the insulator-SC contact. First, Fourier Transform Infrared Spectroscopy (FTIR) in ATR (Attenuated Total Reflection) mode was performed using a diamond crystal [11]. In this configuration, the penetration depth (inverse of absorption coefficient [12]) is between 0.5 and 2 µm according to the wavelength. With this technique the chemical bonds present in the single layer LDPE, known to play an important role in the contact properties [13], present in the single layer LDPE were determined.

To characterize interface properties, the Multimode 8 from Bruker is used. Peak Force Amplitude Modulation Kelvin Probe Force Microscopy (PF-AM-KPFM) is the AFM technique performed. It combines two different modes: Peak-Force Quantitative NanoMechanical (PF-QNM) to probe mechanical properties [14] and Kelvin Probe Force Microscopy (KPFM) to probe surface potential [15]. PF-QNM consists in acquiring topography and mechanical properties (adhesion, deformation, Young modulus…) and KPFM (with fixed cantilever lift from the surface) consists in acquiring the surface potential. The AFM tip has a PtIr coating (SCM-PIT) and nominal spring constant (3±2)N/m. For surface potential measurement a lift of 40 nm is used.

To determine mechanical properties from Peak Force measurement, an AFM-tip calibration is needed. For this, in a first step we determined the photodetector sensitivity using Force Distance Curve Measurement. Then we computed the cantilever spring constant using the Thermal Tune mode [16]. A spring constant of 1.66 N/m was found in this way.

III. Results and Discussion

In this section samples produced with aluminum or PET cover layers will be compared. First, the LDPE was characterized with FTIR, afterwards the SC-LDPE-SC sandwich was investigated with atomic probe microscopies.

A. *FTIR results*

Fig. 2 compares the ATR-FTIR spectra obtained on LDPE single layer processed using either PET or Aluminum cover layers during samples press-molding. Classical LDPE vibration modes are observed for both samples. The essential differences between the two samples are found in the region 1000 to 1800 cm^{-1}. Higher absorption is found at 1722 cm^{-1} and 1263 cm^{-1} for the sample processed with PET. These represent the vibration modes, respectively for double and single carbon-oxygen bonds. This could be interpreted as a more advanced oxidative stage, or more likely to some diffusion of moieties from the PET layer when in contact with the material.

B. *Cross-sections of SC-LDPE-SC sandwiches using different AFM imaging modes*

Two sandwiches, processed with aluminum and PET cover layers, were prepared to characterize the cross-section surface with AFM. The images shown in Fig.3 were obtained on a sample processed with Al as cover layer. They correspond to the 3 modes: topography, mechanical response in adhesion, and surface potential. Note that the three images were realized exactly on the identical sample area during the same measurement. The surface topography map (Fig.3a) shows the height difference between different areas. The topography is not flat, and it is noticeable that the central part, which is slightly hollowed, has a lower height compared to the rest of the sample. The surface topography can also measure the surface roughness. The average roughness takes two different values, about 10 nm for the LDPE and about 20 nm for the SC, due to the protruding dots. Fig.3b corresponds to the surface adhesion map. This quantity gives the greatest contrast between LDPE and SC, which reveals the separation between the two materials. The image clearly shows that there are no defects like voided

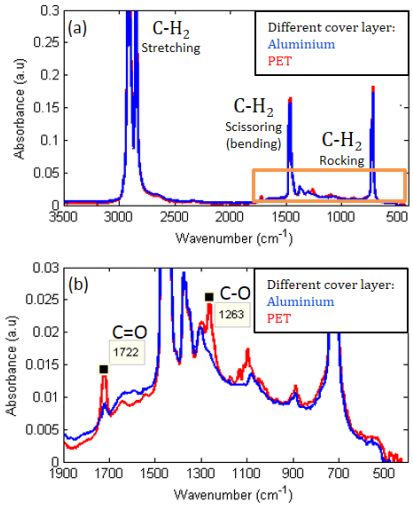

Fig. 2 FTIR spectra of LDPE single layer, using different cover layers, in ATR with a diamond crystal and a internal reflection angle of 45°: (a) full range and (b) details on impurities.

Cite as: F. Gullo, T. Christen, C. Villeneuve-Faure, C. Törnkvist, S. Le Roy, H. Hillborg, C. Laurent, G. Teyssedre, "*Nano-scale characterization of dielectric-semicon contacts*", IEEE Int. Conf. on Dielectrics (ICD), Montpellier, 3-7 July 2016. Proc. ICD, pp. 796-799, **2016**. DOI: 10.1109/ICD.2016.7547735

areas at the interface and that the two materials are smoothly bonded together. Fig. 3c presents the surface potential map and Fig. 3d the potential profile on a line perpendicular to the interfaces (cf. Fig. 3c). The vertical lines on Fig. 3d define the physical interfaces between LDPE and SC as identified from the adhesion map image. Note that according to the Poisson's equation, the space charge density is proportional to the negative second space-derivative (a measure for the curvature) of the potential. The figures show that from the electrical point of view the interface is not as sharp as for the adhesion map, but the potential gradually decreases within LDPE. The potential is almost symmetrical, with the exception of a peak present near the right contact, probably due to a defect close to the surface. In Fig. 3d the potential profile on a line, perpendicular to the interfaces, was added as a reference. The vertical lines define the physical interfaces between LDPE and SC as identified from the adhesion map image.

A similar analysis for the sample prepared using PET cover layer is represented in Fig. 4. The surface topography (Fig.4a) seems smoother compared to the one of Fig. 3a. The adhesion map (Fig. 4b) are however comparable. The main difference in the surface potential map is the existence of an almost zero surface potential in the whole insulator and also in the SC, when the samples are processed PET. For metals the surface potential is usually considered as the work function difference between the AFM tip and the material being probed. For semiconductors, it is the difference with respect to the Fermi levels [17]. The contrast obtained by scanning the surface of heterogeneous materials would then be related to variations in work function or Fermi levels. For organic insulators, however, the interpretation is not so straightforward. Indeed, they are usually considered like semiconductors, but their HOMO-LUMO gap is typically large (for LDPE it is about 8 eV), therefore the concentration of thermally excited carriers is extremely small. The issue of KPFM measurements on insulating surfaces was addressed, e.g., by Ishii et al. [18]. The observed potential reflects the charge distribution in the sample layer and the substrate surface. However, the present results are obtained with the ground on the lateral electrode, which does greatly change the limit conditions. As the potential profiles are through the interface, it may reflect energy level equalization, with charge exchange between the two materials. Sharp profiles have been reported for example in case of PZT/Pt/SiO2 interfaces [19]. The relative spreading of the potential can therefore be related to the spreading of the space charge associated to band bending, or to the specific geometry of the system.

Concerning the difference in potential profiles for the two materials, two possible hypotheses are

- greater surface oxidation in case of PET cover layer, and polarization processes
- impact of the sample thickness: realizing that the sample made with PET cover-layer is substantially thinner (28µm vs. 41µm), two interfaces regions would be in interaction providing a homogenization of the potential, cf. Fig. 3c vs. Fig. 4c.

Previous images were obtained by scanning the surface over a length of 70 µm to give an overview of the sandwich structure. This represents a very large scale for the AFM and a narrower view is presented in Fig.5. At this scale, the SC is no longer uniform, and it is possible to distinguish the CB nanodots in topography (Fig.5.a and 5.c) and adhesion (Fig.5.b and 5.d) maps. What is considered as nanodots or clusters of nanodots appear with less adhesion force compared to the polymeric matrix.

Imaging the surface with greater magnification allows estimating the size of these nanodots or clusters at around 80 nm. The SC-LDPE interface, which appeared flat at bigger scale, now shows an appreciable nano-roughness in adhesion.

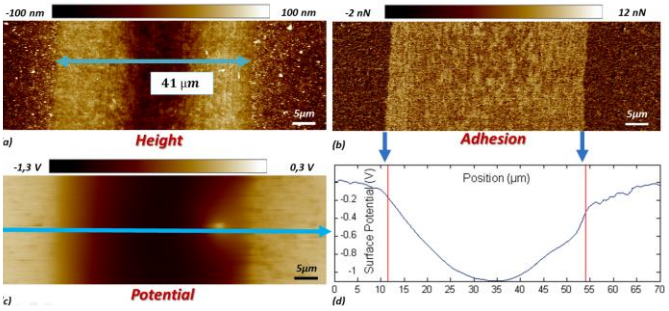

Fig. 3 Images of SC-LDPE-SC cross-sections processed using aluminum cover layer, analyzed with PF-KPFM-AM mode. The maps represent different surface properties: (a) surface topography, (b) surface adhesion, (c) surface potential (d) surface potential on a single line. Vertical lines in (d) are physical interfaces identified by adhesion measurements. The colour bar on maps represents the scale of measured quantities.

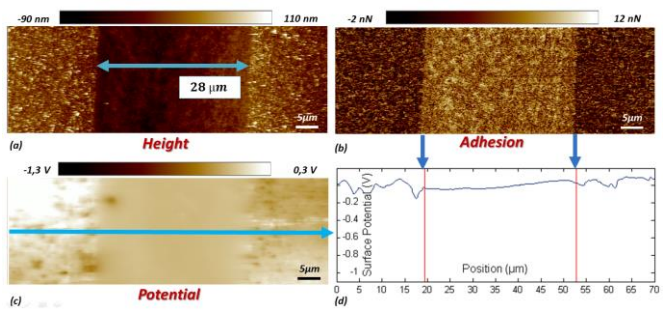

Fig. 4 Images of SC-LDPE-SC cross-sections processed using PET cover layer, analyzed using PF-KPFM-AM mode. The maps represent the same surface properties as described in Fig. 3.

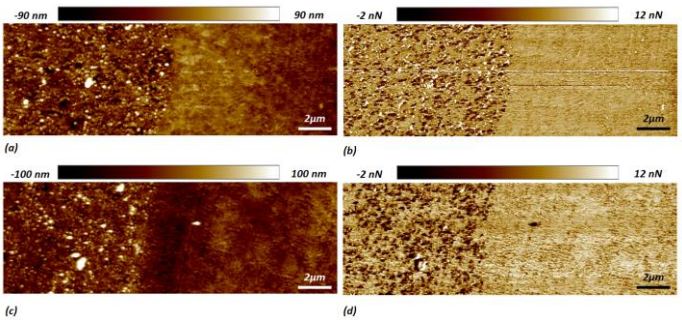

Fig. 5 Zoom on the SC-LDPE interface processed with aluminum (a,b) and PET (c,d) cover layers, and analyzed with PF-KPFM-AM mode. The images represent: (a,c) surface topography, (b,d) surface adhesion.

Cite as: F. Gullo, T. Christen, C. Villeneuve-Faure, C. Törnkvist, S. Le Roy, H. Hillborg, C. Laurent, G. Teyssedre, "*Nano-scale characterization of dielectric-semicon contacts*", IEEE Int. Conf. on Dielectrics (ICD), Montpellier, 3-7 July 2016. Proc. ICD, pp. 796-799, **2016**. DOI: 10.1109/ICD.2016.7547735

This zoom demonstrates that there is no carbon black migration in the LDPE volume. The interface roughness is characterized by peak-to-valley distance around 200 nm. However, considering the current images, the interface between the SC and LDPE appears sharp, without evident accumulation or spreading of the CB at the interface.

IV. CONCLUSIONS

A technique was developed for preparing small SC-LDPE-SC sandwich samples. Their interface roughness profiles were characterized with a peak-to-valley distance of around 200 nm. With an ultra-cryo-microtome, a cross-section surface with an average roughness of less than 20 nm was achieved. For these samples it is possible to characterize the electrode-insulator contact on a microscopic scale, which is of large relevance for HVDC cable insulation with SC-PE interfaces.

The FTIR analysis, suggests that the sample processed using PET as cover-layer presents more oxidized moieties on its surface. Cover-layers are not present during cable and cable accessory production, but they are present during production of small insulation samples, which are usually used for determining the electrical properties of a (new) cable or accessory material. A difference between the samples made with Al and PET cover-layers is also revealed in the surface potential profile. The potential varies smoothly at both interfaces of the sandwich and the shape of the variation points to negative charge build-up over several micrometers within the LDPE layer. From the surface mechanical properties, it is possible to extract information on the sharpness of the interfaces at the larger scales, and on the distribution of CB at the smaller scales. Since the polymer host matrix is the same for SC and insulation, the only way to distinguish the interface is to observe the presence of the nanodots.

In summary, we demonstrated a suitable methodology to perform a comprehensive characterization of an insulator-SC interface down to the nanoscale. Although some significant further effort is needed, this will eventually help us to produce optimized SC-LDPE contacts.

ACKNOWLEDGMENTS

Authors thanks S. Balor of IBCG-biotoul for ultra-cryo-microtomography.

REFERENCES

[1] T. L. Hanley, R. P. Burford, R. J. Fleming, and K. W. Barber, “A general review of polymeric insulation for use in HVDC cables,” IEEE Electr. Insul. Mag., vol. 19, no. 1, pp. 13–24, 2003.

[2] T. Christen, "Characterization and Robustness of HVDC insulation", IEEE Int. Conf. Sol. Diel (ICSD), Bologna, Italy, pp. 238-241, 2013.

[3] T. T. N. Vu, G. Teyssedre, B. Vissouvanadin, S. Le Roy, C. Laurent, M. Mammeri, and I. Denizet, “Electric field profile measurement and modeling in multi-dielectrics for HVDC application,” Proc. IEEE Int. Conf. Solid Dielectr. ICSD, pp. 413–416, 2013.

[4] T. Christen, “HVDC insulation boundary conditions for modeling and simulation,” IEEE Trans. Dielectr. Electr. Insul., vol. 22, pp. 35–44, 2015.

[5] M. Taleb, G. Teyssèdre, S. Roy, and C. Laurent, “Modeling of charge injection and extraction in a metal/polymer interface through an exponential distribution of surface states,” IEEE Trans. Dielectr. Electr. Insul., vol. 20, pp. 311–320, 2013.

[6] G. Teyssedre and C. Laurent, “Charge transport modeling in insulating polymers: From molecular to macroscopic scale,” IEEE Trans. Dielectr. Electr. Insul., vol. 12, pp. 857–874, 2005.

[7] T. Maeno and K. Fukunaga, "High-resolution PEA charge distribution measurement system", IEEE Trans. Dielectr. Electr. Insul., vol. 3, p. 754, 1996.

[8] T. Takada, “Space Charge Measurement in Dielectrics and Insulating Materials”, CIGRE Technical Brochure (TF D1.12.01) No. 288, pp.1-50, 2006.

[9] H. Ghorbani, M. Saltzer, F. Abid, and H. Edin, “Heat-treatment and physical properties of high voltage DC XLPE cable insulation material”, to be published .

[10] H. Ghorbani, “Characterization of conduction and polarization properties of HVDC cable XLPE Insulation Materials”, Licentiate Thesis, KTH, Stockholm, Sweden, 2016.

[11] J. F. Rabek, “Polymer photodegradation: mechanisms and experimental methods“, New York: Springer, pp. 514-515, 1995.

[12] G. R. Fowles, Introduction to Modern Optics, 1975, New York: Dover, 2010

[13] F. Khabbaz, A. Albertsson, and S. Karlsson, “Chemical and morphological changes of environmentally degradable polyethylene films exposed to thermo-oxidation,” Polym. Degrad. Stab., vol. 63, pp. 127–138, 1999.

[14] J. Young, M. A. Monclus, T. L. Burnett, W. R. Broughton, S. L. Ogin, and P. A. Smith, “The use of the PeakForce quantitative nanomechanical mapping AFM-based method for high-resolution Young’s modulus measurement of polymers,” Meas. Sci. Technol., vol. 22, p. 125703, 2011

[15] U. Zerweck, C. Loppacher, T. Otto, S. Grafström, and L. M. Eng, “Accuracy and resolution limits of Kelvin probe force microscopy,” Phys. Rev. B, vol. 71, p. 125424, 2005.

[16] J. L. Hutter and J. Bechhoefer, “Calibration of atomic-force microscope tips,” Rev. Sci. Instrum., vol. 64, no. 7, pp. 1868–1873, 1993.

[17] M. Ishii, “Static states and dynamic behaviour of charges: observation and control by scanning probe microscopy.,” J. Phys. Condens. Matter, vol. 22, no. 17, p. 173001, 2010.

[18] H. Ishii, N. Hayashi, E. Ito, Y. Washizu, K. Sugi, Y. Kimura, M. Niwano, O. Ouchi, and K. Seki, “Kelvin Probe Study of Band Bending at Organic Semiconductor / Metal Interfaces : Examination of Fermi Level Alignment,” Phys. Stat. Sol. a, vol. 201, pp. 1075-1094, 2004.

[19] L. M. Eng, "Nanoinspection of Dielectric and Polarization Properties at Inner and Outer Interfaces in Functional Ferroelectric PZT Thin Films." Scanning Probe Microscopy: Characterization, Nanofabrication and Device Application of Functional Materials, Springer, Netherlands, pp. 275-287, 2005.

Cite as: F. Gullo, T. Christen, C. Villeneuve-Faure, C. Törnkvist, S. Le Roy, H. Hillborg, C. Laurent, G. Teyssedre, *"Nano-scale characterization of dielectric-semicon contacts"*, IEEE Int. Conf. on Dielectrics (ICD), Montpellier, 3-7 July 2016. Proc. ICD, pp. 796-799, **2016**. DOI: 10.1109/ICD.2016.7547735